Junction Point Fluctuations in Microphase Separated Polystyrene−Polyisoprene−Polystyrene Triblock Copolymer Melts. A Dielectric and Rheological Investigation

I. Alig[†] and G. Floudas*

Foundation for Research and Technology-Hellas (FORTH), Institute of Electronic Structure and Laser, P.O. Box 1527, 711 10 Heraklion, Crete, Greece

A. Avgeropoulos and N. Hadjichristidis

Department of Chemistry, University of Athens, Panepistimiopolis, Zografou,15771 Athens, Greece, and Foundation for Research and Technology−Hellas, Institute of Electronic Structure and Laser, P.O. Box 1527, 711 10 Heraklion, Crete, Greece

Received January 27, 1997; Revised Manuscript Received May 22, 1997[⊗]

ABSTRACT: Dielectric spectroscopy is employed in two polystyrene−polyisoprene−polystyrene (SIS) triblock copolymers well below the order-to-disorder transition temperature and in the frequency range from 10^{-2} to 10^{6} Hz. Small angle X-ray scattering has shown the formation of lamellar structures with a long period of about 25 nm. Besides the polyisoprene and polystyrene segmental relaxations and a slower process associated with the reorientation of the interface, we provide evidence for a new type of chain dynamics associated with the mobility of the junction points at the interface. From the relaxation strength of this process—which is very much reduced as compared to the chain relaxation in bulk polyisoprene—we extract a characteristic length of the end-to-end vector fluctuations in the interface in the range 4−6 nm. This value compares well with an independent estimate of the interfacial thickness based on thermodynamics. Dielectric spectroscopy can therefore be used as a *dynamic probe of the interface* in ordered triblock copolymers. Over the same temperature range rheology is influenced by a broad spectrum of modes related to the dynamics of tethered polyisoprene chains.

I. Introduction

Block copolymers have attracted a lot of attention mainly because of their ability to form unique nanostructures whose phase and size can be controlled at the synthesis level.[1] Such materials find applications as surfactants, adhesives, and compatibilizers of polymer blends. Key factors for their important applications are the interfacial properties of the two polymers. As a result, there has been a lot of theoretical effort to calculate parameters such as the surface tension and the interfacial thickness. For example, the interfacial thickness between two immiscible homopolymers was calculated in the limit of long homopolymers by Helfand and co-workers[2] as

$$\Delta_\infty = \frac{2a}{\sqrt{6\chi}} \tag{1}$$

where a is the statistical segment length (assuming $a_A = a_B = a$) and χ is the interaction parameter. Equation 1, correctly predicts the interfacial thickness in block copolymers only in the strong segregation limit ($\chi N >> 10$, where N is the total degree of polymerization). The effect of the finite molecular weight of the homopolymers is to increase Δ which now depends on the block incompatibility[3]

$$\Delta \approx \Delta_\infty\left[1 + \ln 2\left(\frac{1}{\chi N_A} + \frac{1}{\chi N_B}\right)\right] \tag{2}$$

where N_A, N_B are the degrees of polymerization of the A and B homopolymers, respectively. Corrections due to the connectivity of blocks were found to be significant and resulted in a broader interface[4]

$$\Delta \approx \Delta_\infty\left[1 + \frac{1.34}{(\chi N)^{1/3}}\right] \tag{3}$$

Based on the above equations, a typical interfacial thickness for a phase-separated polystyrene−polyisoprene diblock copolymer with $N = 1000$, $\chi \approx 0.1$, and $a \approx 0.68$ nm is about 2.2 nm. In addition to the usual applications of most block copolymers, triblock copolymers such as polystyrene−polyisoprene−polystyrene (SIS) can be considered as thermoplastic elastomers, a property which results here from tethering both ends of the rubbery block to the glassy PS domains.

Molecular architecture plays an important role in determining the phase behavior and the viscoelastic properties of block copolymers.[5−8] The phase stability criteria and structure factor in the disordered phase have been calculated first for diblock copolymers[5] and later for triblock copolymers in the context of the mean-field theory (MFT).[9−11] The critical value of the product χN increases from 10.5 for symmetric diblock copolymers to 18 for the triblock case. Furthermore, as with diblock copolymers, fluctuation corrections to the triblock MFT phase diagram[11] result in the destruction of the less stable phases and open channels in composition for direct transitions from the lamellar to the disordered phase.

The rheological behavior of triblock copolymers has been examined for lamellar,[12−15] cylindrical,[12,16−22] and spherical[12,23] structures. It is widely recognized that a factor which influences the viscoelastic properties of triblock copolymers is the ratio of loops vs bridges of the PI mid-block. An answer to this problem was given recently[24] by dielectric spectroscopy on SIS triblocks with a dipole inversion in the middle block. Dielectric

[†] Deutsches Kunststoff-Institut, Schlossgartenstrasse 6, D-64289 Darmstadt, Germany.

[⊗] Abstract published in *Advance ACS Abstracts,* August 1, 1997.

S0024-9297(97)00101-0 CCC: $14.00

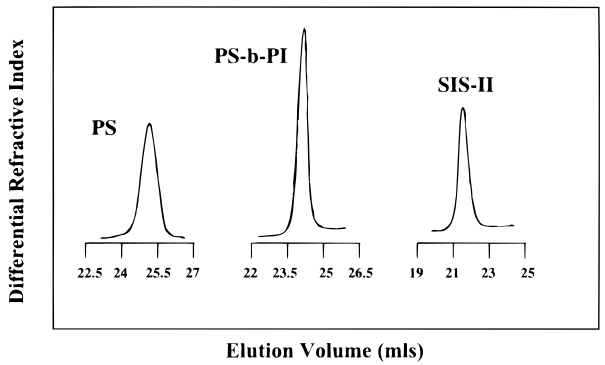

Figure 1. SEC chromatographs of the precursors and the final triblock copolymer SIS-II.

spectroscopy (DS) is a powerful technique in studying the local and global dynamics of polymers possessing dipoles perpendicular and parallel to the chain contour, respectively. The DS on polymers with dipoles aligned parallel to the chain contour (called type-A) was pioneered by Stockmayer[25] and studied extensively by several groups.[26] These studies have shown that polyisoprene (PI) is an ideal type-A polymer mainly due to the high cis-content.

In the present study we investigate the dynamics in two lamellar forming SIS triblock copolymers using dielectric spectroscopy and rheology. Our DS results provide evidence for a mobile PS−PI (polystyrene−polyisoprene) junction point which can be used as a *dynamic probe* of the interface. Rheology provides the spectrum of modes corresponding to entangled PI chains which are compared to the DS results.

II. Experimental Section

Materials. The triblock copolymers were prepared by anionic polymerization using high vacuum techniques in evacuated, *n*-BuLi washed, and benzene-rinsed glass vessels. The purification of styrene (Merck), isoprene (Fluka), and benzene (Merck) to the standards required for anionic polymerization have been described elsewhere.[27−29] Tetrahydrofuran (THF, Merck) was stirred overnight over CaH_2, distilled to a sodium mirror, and left to react for 24 h. The procedure was repeated until no degradation of the mirror was observed. Finally it was distilled in an alloy of potassium/sodium (3/1), where the formation of blue color occurred. The triblock copolymers were synthesized by sequential addition of the monomers according to the following reaction scheme:

$$\mathrm{St} + \text{sec-BuLi} \xrightarrow{C_6H_6} \mathrm{PS^{(-)}Li^{(+)}}$$

$$\mathrm{PS^{(-)}Li^{(+)}} + \mathrm{Is} \xrightarrow{C_6H_6} \mathrm{PSPI^{(-)}Li^{(+)}}$$

$$\mathrm{PSPI^{(-)}Li^{(+)}} + \mathrm{St} \xrightarrow[\text{small amount of THF}]{C_6H_6} \mathrm{PSPIPS}$$

PSPIPS: triblock copolymer of the ABA type

In the last step a small amount of THF (0.5 mL) was added to accelerate the initiation rate of the styrene toward the polyisoprenyllithium macroinitiator. Since the THF is added after the completion of the polymerization of isoprene, no change in the microstructure occurred. All steps were monitored by size exclusion chromatography, SEC (Figure 1). SEC experiments were carried out at 30 °C using a Waters (Model 510) pump, Waters (model 410) differential refractometer and Waters (model 486) tunable absorbance detector. Three Phenomenex (phenogel 5 linear, pore size 50 to 10^{-6} Å) columns were used. THF distilled over CaH_2 and sodium was the carrier solvent, at a flow rate of 1 mL/min. The weight average molecular weight ($\bar{M}_w$) of the final polymers was determined with a Chromatix KMX-6 low-angle laser photometer (LALLS) operating at 633 nm. THF purified over CaH_2 and sodium distilled prior to use was used as the solvent at 25 °C. The number average molecular weight ($\bar{M}_n$) was determined with a Wescan (Model 230) membrane osmometer at 35 °C. Toluene, distilled over CaH_2, was the solvent. The $\bar{M}_w$ values were obtained from the $(KC/\Delta R_\theta)^{1/2}$ vs C plots (ΔR_θ is the excess Rayleigh ratio, K is a constant, and C is the concentration) and the $\bar{M}_n$ values from the $(\Pi/C)^{1/2}$ vs C plots (Π is the osmotic pressure). In all cases the correlation coefficient was better than 0.99. ^{1}H-NMR was used for the determination of the composition and the microstructure of the materials in $CDCl_3$ at 30 °C using a Varian Unity Plus 300/54 instrument. For the polyisoprene block, the typical microstructure characteristic of anionic polymerization of isoprene in benzene was observed (9 wt % 3,4, 70 wt % *cis*-1,4 and 21 wt % *trans*-1,4). More details concerning the SEC, LALLS, membrane osmometry (MO), and ^{1}H-NMR measurements are given elsewhere.[28,29] The molecular characteristics of the triblock copolymers and of the homopolymers used in the present study are shown in Table 1.

Table 1. Characteristics of the PS−PI−PS Triblock Copolymers and the Homopolymers (PS, PI) Used in the DS Studies

sample	$10^{-3}\,\bar{M}_n$[a]	$10^{-3}\,\bar{M}_w$[b]	$\bar{M}_w/\bar{M}_n$[c]	% PS[d]	f_{PS}[f]
SIS-I	65.0	68.1	1.05	64	0.6
SIS-II	72.1	76.5	1.06	59	0.55
PI	10.5	10.8	1.03	0	0
PS	16.7	17.0	1.02	100	1

[a] Membrane osmometry (toluene, 35 °C). [b] Low-angle laser light scattering (THF, 25 °C). [c] SEC (THF, 30 °C). [d] ^{1}H-NMR. [f] Calculated from $N_n = N_{n,PS}^* + N_{n,PI}^* = N_{n,PS}(\rho_I^*/\rho_S^*)^{1/2} + N_{n,PI}(\rho_S^*/\rho_I^*)^{1/2}$ and $f_{PS} = N_{n,PS}^*/N_n$, where $N_{n,i}$ are the degrees of polymerization of each block and ρ_i^* are the molar densities.

Small-Angle X-ray Scattering (SAXS). The morphology of the shear-oriented sample (see below) was investigated using a 18 kW rotating anode as the X-ray source (Rigaku) with a pinhole collimation and a two-dimensional detector (Siemens) with 512 × 512 pixels. A double graphite monochromator for the Cu Kα radiation ($\lambda = 0.154$ nm) was used, and three pinholes prior to the sample resulted in a beam diameter of about 1 mm. The sample-to-detector distance was 1.2 m. The scattering patterns from the radial, tangential, and normal views of the SIS-II are shown in Figure 2 and indicate a lamellar structure with a long period of 25.6 nm.

Dielectric Spectroscopy (DS). Measurements of the complex dielectric function have been made with a Novocontrol BDC-S system composed of a frequency response analyzer (Solartron Schlumberger FRA 1260) and a broad band dielectric converter with an active sample cell. The latter contains six reference capacitors in the range from 25 to 1000 pF. Measurements were made in the frequency range from 10^{-2} to 10^6 Hz using a combination of three capacitors in the active sample cell. The resolution in tan δ was about 2×10^{-4} in the frequency range between 10^{-1} and 10^5 Hz. The samples were kept between two gold-plated stainless steel plates of 30 mm diameter with a separation of 100 μm which resulted in a sample capacitance of about 100 pF. The sample cell was set in the cryostat and the sample temperature was controlled between 213 and 413 K and measured with a PT100 sensor in the lower plate of the sample capacitor with an accuracy of ±0.1 K. Typical dielectric loss curves for the SIS-I triblock are shown in Figure 3, in a 3-D representation.

Rheology. An advanced rheometric expansion system (ARES) equipped with a force-rebalanced transducer was used in the oscillatory mode. Different types of experiments have been performed. First, the linear and nonlinear viscoelastic ranges were identified, by recording the strain amplitude dependence of the complex shear modulus G^*. The only experiment with a strain amplitude corresponding to the nonlinear viscoelastic range was made to induce orientational order in the material by applying large amplitude oscillations at $T = 398$ K with a frequency of 1 rad/s and with a strain amplitude of 50%. The sample was subsequently quenched to ambient temperature and examined with the two-dimensional detector (Figure 2). In the remaining experiments strain amplitudes within the linear viscoelastic range were

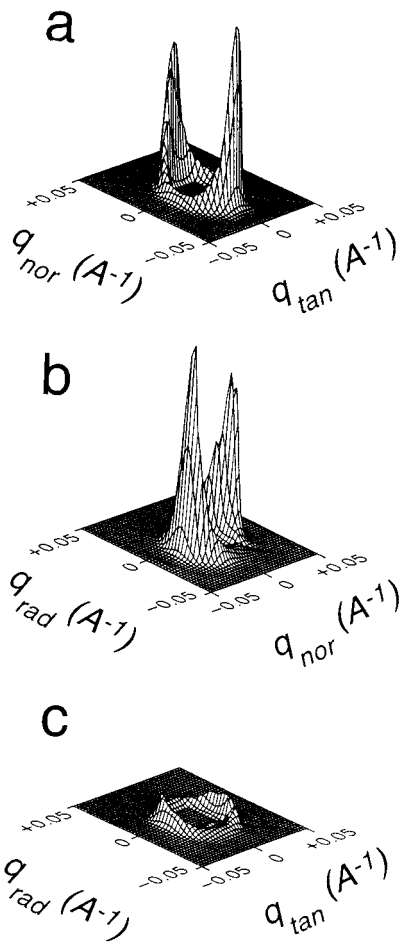

Figure 2. SAXS patterns of the SIS-II triblock copolymer taken with a two-dimensional detector at $T = 300$ K from a sample which has been shear oriented at 398 K. The radial (a), tangential (b), and normal (c) views are shown and indicate the formation of a lamellar structure.

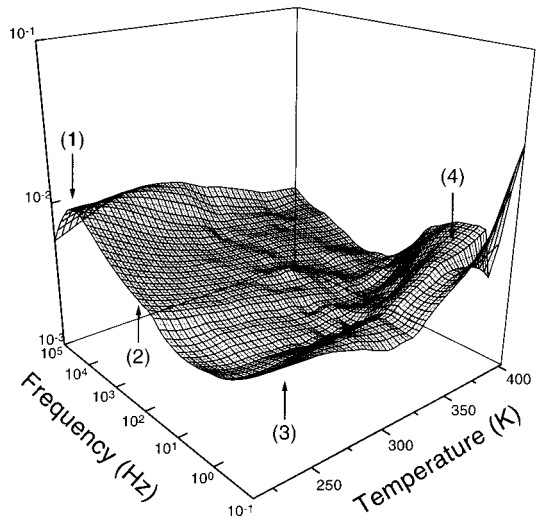

Figure 3. Frequency and temperature dependence of the dielectric loss for the triblock SIS-I showing (1) the PI segmental relaxation, (2) a broad mode associated with the suppressed chain relaxation (see text), (3) a PS-like process, and (4) a slower mode in addition to the conductivity contribution at higher temperatures.

used. These experiments involved (i) isochronal temperature scans within the range 300−543 K aiming to identify the order-to-disorder transition temperature T_{ODT} and possibly an order-to-order transition and (ii) isothermal frequency scans for temperatures in the range 300−443 K and for frequencies $10^{-2} < \omega < 10^{2}$ rad/s. From the isochronal temperature scans we concluded that the T_{ODT} in the triblock copolymer is not within an accessible T-range and that there is no indication for an order-to-order transition within the investigated temperature range.

III. Data Analysis

The dielectric data are discussed in terms of the complex dielectric permittivity $\epsilon^* = \epsilon' - i\epsilon''$, where ϵ' is the real and ϵ'' the imaginary part, which is a function of frequency ω and temperature T, i.e., $\epsilon^* = \epsilon^*(\omega,T)$. Within the investigated frequency range we can assume that mainly two principal mechanisms contribute to ϵ^* arising from the orientation polarization of permanent electrical dipoles (ϵ^*_{dip}) and from the dc conductivity contribution (ϵ^*_{dc})

$$\epsilon^* = \epsilon^*_{dip} + \epsilon^*_{dc} = \epsilon^*_{dip} - i\frac{\sigma_{dc}}{\epsilon_0\omega} \tag{4}$$

The later is caused by free charge carriers, where σ_{dc} is the dc conductivity and $\epsilon_0 = 8.854$ pF/m is the permittivity of free space. In Figure 3, the rise of $\epsilon''(\omega)$ at low frequencies is caused by the electrical conductivity in the material and it is fitted according to $\epsilon_{dc}'' \sim (\sigma_{dc}/\epsilon_o)\omega^{-1}$, where σ_{dc} is considered as a fitting parameter. The orientation polarization contribution of polymers having dipoles perpendicular and parallel to the chain contour can be subdivided further in processes involving local and global (chain) modes as discussed below.

The orientational relaxation contribution to the complex dielectric permittivity of a macroscopic system can be expressed by the Fourier−Laplace transform of the time derivative of the normalized response function $\Phi(t)$ of the polarization $\mathbf{P}(t)$ of the system

$$\frac{\epsilon^*_{dip}(\omega) - \epsilon_\infty}{\Delta\epsilon} = \int_0^\infty e^{-i\omega t}\left(-\frac{d\Phi}{dt}\right) dt \tag{5}$$

where ϵ_0 and ϵ_∞ are the limiting low- and high-frequency permittivities, respectively, and $\Delta\epsilon$ ($=\epsilon_0 - \epsilon_\infty$) is the relaxation strength. $\Phi(t)$ is given by

$$\Phi(t) = \frac{\langle \mathbf{P}(t)\cdot\mathbf{P}(0)\rangle}{\langle \mathbf{P}(0)\cdot\mathbf{P}(0)\rangle} \tag{6}$$

and the polarization $\mathbf{P}(t)$ is given by the sum of all dipoles in the system. $\Phi(t)$ can be decomposed into two components: one related to dipole moments parallel to the chain contour ($\mu^{\parallel}$) and another to dipole moments perpendicular to the chain contour ($\mu^{\perp}$), thus giving rise to the global normal mode and the local segmental relaxation, respectively. In general, $\mathbf{P}(t)$ contains intra- and intermolecular contributions. However, measurements of the dielectric strength as a function of polymer concentration in solutions of cis-PI in a theta solvent (dioxane) up to the bulk revealed that intermolecular dipole−dipole interactions are negligible.[26c] Moreover, assuming that the time scales are very different, we can ignore the cross terms between the parallel and perpendicular components:

$$\Phi(t) = \frac{\sum_j\sum_m \langle \mu^{\parallel}{}_{ij}(0)\cdot\mu^{\parallel}{}_{im}(t)\rangle + \sum_j\sum_m \langle \mu^{\perp}{}_{ij}(0)\cdot\mu^{\perp}{}_{im}(t)\rangle}{\sum_j\sum_m \langle \mu^{\parallel}{}_{ij}(0)\cdot\mu^{\parallel}{}_{im}(0)\rangle + \sum_j\sum_m \langle \mu^{\perp}{}_{ij}(0)\cdot\mu^{\perp}{}_{im}(0)\rangle} \tag{7}$$

For a Gaussian chain the parallel component in $\Phi(t)$

corresponds to the end-to-end vector motion

$$\sum_j \sum_m \langle \mu^{\parallel}_{ij}(0) \cdot \mu^{\parallel}_{im}(t) \rangle = \mu^2 \langle \mathbf{r}_i(0) \cdot \mathbf{r}_i(t) \rangle \qquad (8)$$

Since the relaxation times of the two components present in $\Phi(t)$ are well separated in the time domain, the individual autocorrelation functions can be calculated. From eqs 5−8 the complex dielectric permittivity ϵ^* due to the normal mode process is given by

$$\frac{\epsilon^*(\omega) - \epsilon_\infty}{\Delta\epsilon} = \frac{1}{\langle r^2 \rangle} \int_0^\infty e^{-i\omega t} \left[- \frac{d\langle \mathbf{r}(0) \cdot \mathbf{r}(t) \rangle}{dt} \right] dt \qquad (9)$$

where $\langle r^2 \rangle$ denotes the mean square end-to-end distance and $\Delta\epsilon_n$ ($=\epsilon_0 - \epsilon_{\infty,n}$) is here the relaxation strength for the normal mode process, with $\epsilon_{\infty,n}$ being the high frequency limit of this process.

The analysis of the DS spectra was based on the empirical equation of Havriliak and Negami (HN)

$$\frac{\epsilon_{dip}^*(\omega) - \epsilon_\infty}{\Delta\epsilon} = \frac{1}{[1 + (i\omega\tau_{HN})^\alpha]^\gamma} \qquad (10)$$

where τ_{HN} is the characteristic relaxation time in this equation. The parameters α and γ describe, respectively, the symmetrical and asymmetrical broadening of the distribution of relaxation times. In a log ϵ'' vs log f plot, α and $\alpha\gamma$ give respectively the low- and high-frequency slopes of the relaxation function.

IV. Results and Discussion

Dielectric Spectroscopy. The information provided by the static experiments on the morphology (Figure 2) was that both triblock copolymers formed lamellar structures with long periods of 24.6 and 25.6 nm for the SIS-I and SIS-II, respectively. The dielectric measurements were made on unoriented samples but at temperatures much below the order-to-disorder transition. The 3-D representation of the dielectric loss for the sample SIS-I (Figure 3) shows the existence of multiple relaxation processes in addition to the conductivity contribution at high temperatures/low frequencies. Starting from low temperatures, the spectrum is influenced by the local segmental dynamics of PI (process 1). At a temperature range where the normal mode process of bulk PI is expected, there is a much broader process with reduced intensity (process 2). At higher temperatures, in the vicinity of the PS glass transition, there is a PS-like process (process 3) and at even higher temperatures a slower process associated with the reorientation of the interface (process 4). All but the second process were expected from previous experiments on microphase separated diblock copolymers.[26] In this study we focus therefore on the second process.

To demonstrate the existence of this process, we rely separately on temperature and frequency representations, respectively, in Figures 4 and 5. In Figure 4, the temperature dependence of the dielectric loss from the two triblock copolymers is compared with those of PI and PS homopolymers (Table 1). Evidently, the amplitudes of the local segmental processes correspond to the bulk polymers weighted by composition. Furthermore, there is only a slight shift of the PI local dynamics (in SIS-II), indicating only a small mixing effect at the segmental level. The comparison of the intermediate mode in the triblocks with bulk PI clearly shows the existence of a new very broad mode with suppressed

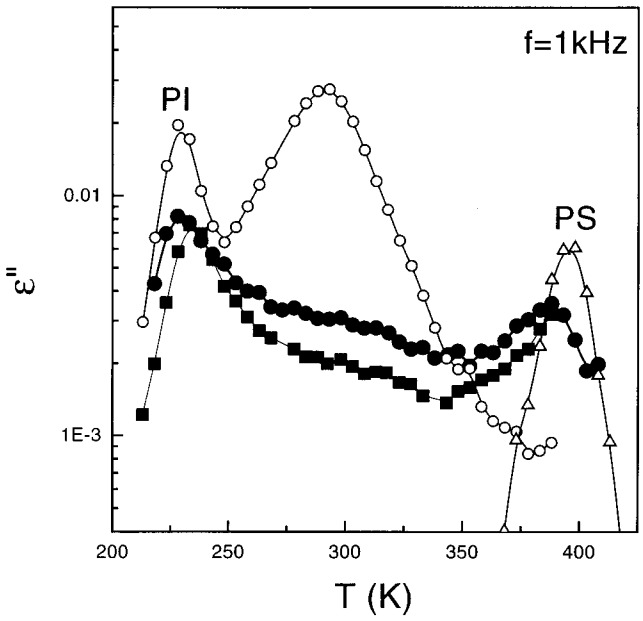

Figure 4. Temperature dependence of the dielectric loss for the triblock copolymers SIS-I (●) and SIS-II (■) and the homopolymers PI (○) and PS (△) at a frequency of 1 kHz.

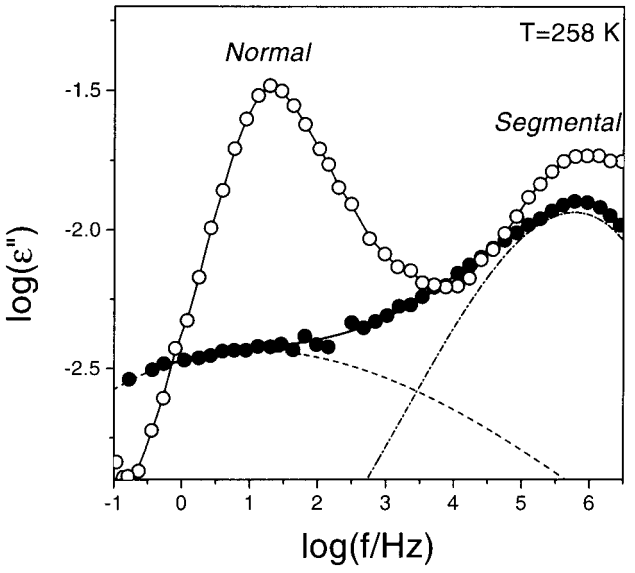

Figure 5. Frequency dependence of the dielectric loss of the triblock copolymer SIS-I (●) compared with that of PI (○) at the same temperature $T = 258$ K. The normal and segmental modes of the bulk PI are indicated. The dashed and dashed-dotted curves are the result from the fit to the normal-mode-like and segmental processes, respectively. The solid line is the sum of the two contributions.

intensity, which, because of its location being in the vicinity of the normal mode of bulk PI, it is assumed to reflect restricted chain motions which can be envisioned as a normal mode-like process. Similarly, in the frequency representation of Figure 5, the segmental relaxation in the triblocks is followed by a slower mode at lower frequencies. Because of the broadness of this mode, in analyzing the dielectric loss data (Figure 5) we have fixed the low- and high-frequency slopes of the segmental process to the corresponding parameters in bulk PI and obtained the distribution parameters of the slower process ($\alpha \approx 0.25$ and γ in the range from 0.6 to 1). These parameters are indicative of a very broad process. The uncertainty in extracting these parameters is about 10% for the two shape parameters and about 20% for the strength of the process. The relax-

Scheme 1

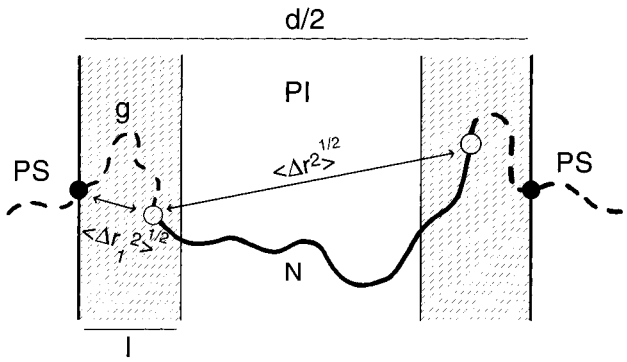

ation times extracted from the fits to eq 10 are plotted in Figure 6 and compared with the local segmental modes of bulk PI (dash-dotted) and PS (solid line) and with the corresponding normal mode of PI (dashed line). In the same plot we include the times obtained from rheology which will be discussed later. In the next section we account for the origin of the broad process.

The dielectric relaxation strength of a type-A polymer for the end-to-end fluctuations, $\langle \Delta r^2 \rangle$, is generally expressed as

$$\Delta\epsilon = \frac{C 4\pi N_A \mu^2 \langle \Delta r^2 \rangle}{3 k_B T \quad M} \tag{11}$$

where C is the concentration of chains, N_A is Avogadro's number, μ is the dipole moment per contour length, and M is the molecular weight of the chain. In the above equation, $\langle \Delta r^2 \rangle = \langle \Delta(\mathbf{r_1} - \mathbf{r_2})^2 \rangle = \langle (\mathbf{r_1} - \mathbf{r_2})^2 \rangle - \langle (\mathbf{r_1} - \mathbf{r_2}) \rangle^2$, where $\mathbf{r_1}$ and $\mathbf{r_2}$ are the two end-vectors assuming that the spatial distribution function of the end-to-end vector is nearly Gaussian. In the special case of a Gaussian chain, $\langle \mathbf{r_1} - \mathbf{r_2} \rangle = 0$, and eq 11 relates the relaxation strength of the longest normal mode to the mean-square end-to-end vector $\langle r^2 \rangle$ ($= \langle (\mathbf{r_1} - \mathbf{r_2})^2 \rangle$).

For an infinitely thin interface without mobility of the junction points parallel to the interface (e.g., due to restrictions caused by entanglements), no dielectrically active relaxation of the end-to-end vector is expected since both ends are tethered. However, in block copolymers there is a finite interfacial thickness given by eqs 1−3. This situation for a triblock copolymer is schematically shown in Scheme 1.

The junction point located at $\mathbf{r_1}$ (open circle) is allowed to fluctuate at the PS-PI interface (shadowed area). The portion of the PS chain, composed of an average number of g segments entering the interface, is effectively tethered on the one side by the glassy PS at the position $\mathbf{r_t}$ (filled circle). Assuming a Gaussian distribution for the subchain between $\mathbf{r_t}$ and $\mathbf{r_1}$ composed of g PS segments, we can calculate the mean-square distance between $\mathbf{r_1}$ and $\mathbf{r_t}$ as $\langle \Delta r_1^2 \rangle = g a_{PS}^2$. Similarly, the mean-square end-to-end distance of the PI block is given by $\langle \Delta r^2 \rangle = N a_{PI}^2$, where N is the number of PI segments. Thus, the value of $\langle \Delta r_1^2 \rangle^{1/2}$ can be considered as the characteristic length of fluctuations of the junction point within the interface. Intrinsic in our simple model is the idea that the PS subchain entering the interface is plasticized by the presence of PI. In general, there will be a distribution of PS segments entering the interface whose mean value is controlled by the interaction parameter ($g \sim \chi^{-1}$).

For each PI block of the SIS triblock copolymer the fluctuations of both end-points of the PI chain have to be considered, i.e., $\langle \Delta r^2 \rangle = 2\langle \Delta r_1^2 \rangle$. Then the characteristic length of the dynamically probed interface is related to the measured strength of this process by:

$$\langle \Delta r_1^2 \rangle = \frac{3 k_B T M_{PI} \Delta\epsilon}{4\pi C N_A \mu^2 2} \tag{12}$$

It is evident that the ratio of the relaxation strength of this process to the normal mode of a free PI chain composed of N segments is $2g/N$ (here we have made the usual mean-field assumption of equal segment lengths, i.e., $a_{PS} \approx a_{PI}$). Therefore, the expectation is that the intensity of this mode will be very much reduced as compared to a free PI chain.

We can now proceed in estimating the theoretical interfacial thickness Δ (eqs 1−3) and the number of PS segments, g, entering the interface, from the interaction parameter χ. The appropriate way to extract $\chi(T)$ in block copolymers is to bring the system in the disordered state (by heating) and there apply the MFT[9−11] with or without fluctuation corrections. For the two triblock copolymers studied here, it was not possible to reach the disordered state without decomposing the samples (we have studied temperatures up to 540 K); therefore we are obliged to use literature values from other SIS triblock copolymers. To our knowledge, one such study exists for triblock copolymer melts with an ordered state morphology consisting of PS spheres embedded on a PI matrix.[23] Since $g \sim \chi^{-1}$, the prediction is that 8−10 PS segments per junction point are entering the interface. Furthermore, we can use eqs 1−3 and $a = 0.68$ nm to estimate the interfacial thickness. The result for Δ_∞ from eq 1 is 1.7 nm which with the corrections for the finite molecular weight and the connectivity of blocks (eqs 2−3) results in about 2.4 nm for the SIS-I. This estimate of the interfacial thickness can now be compared with the result from eq 12, using the measured dielectric strength of the process under investigation, which at $T = 300$ K results in $\langle \Delta r_1^2 \rangle^{1/2} \approx 5-6$ nm. Another estimate of Δ can be provided from the ϵ'' values at a fixed T ($T \approx 300$ K) (Figure 4) by applying again eq 12. The result is about 4 nm. Therefore, the estimated end-to-end vector fluctuations within the interface is 4−6 nm and compares favorably with the estimate based on the thermodynamics if we consider that the thickness of 2.4 nm refers to the half-width of the interface.

Similar arguments can be used for the dynamics of the junction point. The dynamics of the junction point is considered to be dominated by the PS subchain entering the interface which is tethered by the glassy PS domain. Then, the slowest relaxation time can be estimated from $\tau_g \approx 4\zeta_{eff}\, g^2$, where ζ_{eff} is an effective friction coefficient created by the PI and PS segments at the interface and the factor 4 is the usual factor for a tethered chain. Now, a calculation of the junction point dynamics relative to the normal mode time of a free PI chain composed of N segments is possible. This ratio is $\tau_g/\tau_N \approx (\zeta_{eff}/\zeta_{PI})(g/N)^2$. The lower limit of this ratio is practically $(g/N)^2$. Based on the estimation of g from the interaction parameter the expectation, is that, $\tau_g/\tau_N << 1$. As shown in Figure 6, the relaxation times for this mode (solid symbols) are generally faster than those from the normal mode time of a free PI chain (dashed line). A more quantitative comparison is not possible—as can be seen from Figures 4 and 5—because of the very broad distribution of relaxation times which originates both from a distribution of the number of

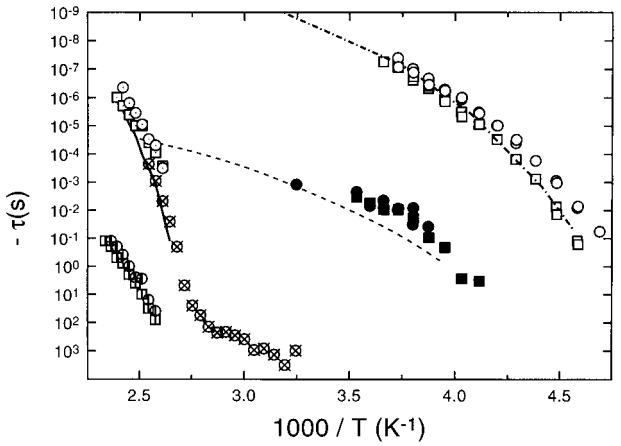

Figure 6. Relaxation map of SIS-I (circles) and SIS-II (squares) in the usual Arrhenius representation: open symbols, PI segmental relaxation (DS); filled symbols: PI chain mode (DS); (open box and circle with center line) slow processess (rheology, obtained from the crossing of G' and G''); (⊗) scaled shift factors for SIS-I (rheology); (open box and circle with center dot) PS-like process in SIS-I and SIS-II, respectively (DS). The dielectric segmental (dash-dotted line) and normal mode (dashed line) times of homopolyisoprene are shown together with the segmental relaxation of bulk polystyrene (solid line).

segments g and of $\zeta_{\text{eff}}(\mathbf{r_1})$ at the interface. Furthermore, it is expected that the gradient in the local friction and the topological constraints lead to an asymmetric spatial distribution function of the junction point fluctuations $\Phi(\mathbf{r_1})$ (which is different from the distribution function of the end-to-end vector for a Rouse chain).

The characteristic times of the slow DS process (which are omitted from Figure 6 for clarity) display a weaker T-dependence as compared to the PS-like processes. This slow mode was discussed in ref 26h; it is a general feature of *ordered* block copolymers with an amplitude which strongly depends on the sample preparation. Because of these features it was assigned to the slow reorientation of the interface formed in the ordered state.

Rheology

The isochronal measurements (not shown here) of the dynamic elastic (G') and loss (G'') moduli showed no evidence for an order-to-disorder transition, up to 540 K. Therefore, both triblocks remain in the ordered phase, within the investigated temperature range. Subsequently, the frequency dependence of the moduli was investigated and the results of the attempted time−temperature superposition (TTS) are shown in Figures 7 and 8, for SIS-I and SIS-II, respectively. Before we discuss the results shown in the figures we need to comment on the applicability of TTS in our systems. TTS is known to be valid for thermorheologically simple systems, i.e., homopolymers, and its application to inhomogeneous microphase separated systems is questionable. Furthermore, one should be aware that the thus obtained shift factors refer to a two phase system whose component solubility generally depends on temperature. This last effect should be more pronounced near the order-to-disorder transition (weak segregation). The triblock copolymers employed here are characterized by an incompatibility parameter, $\chi N \approx 70$, and thus can be considered as strongly segregated. Moreover, we mainly focus on changes occurring in the vicinity of the polystyrene T_g, which we choose as our reference temperature.

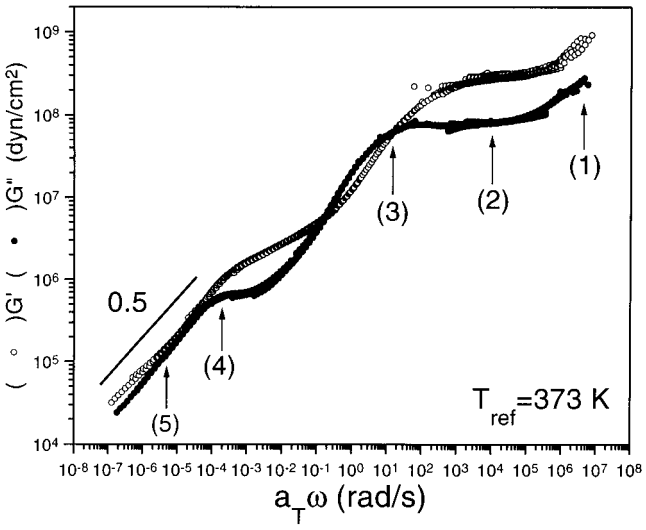

Figure 7. Reduced frequency plot for the storage (○) and loss (●) moduli of the triblock SIS-I shifted to the data at 373 K. The different processes are indicated with arrows and are explained in the text. The shift factors used for the G'' data are given in Figure 9.

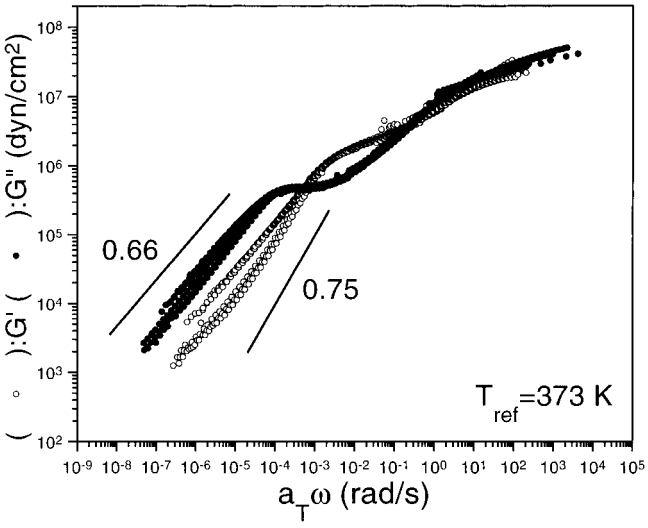

Figure 8. Reduced frequency plot for the storage (○) and loss (●) moduli of the triblock SIS-II shifted to the data at 373 K. The shift factors used for the G'' data are given in Figure 9.

In the master curves shown in Figures 7 and 8, there are different regimes which reflect the multiple length scales (segment, chain, domain, grain) in the microphase separated systems. These different regimes are identified in Figure 7 with arrows, which, starting from low T/high frequencies correspond to (1) the low-frequency side of the the PI glass−rubber relaxation (which corresponds to the PI segmental relaxation measured by DS), (2) a PI plateau dominated by the dynamics of entangled and tethered PI chains, and (3) the PS glass−rubber relaxation (also found by DS) and two processes at higher temperatures indicated as (4) and (5), associated with the ordered structure. The characteristic times from process 4 (obtained in the isothermal measurements by the crossing of G' with G'') compare favorably with the slow DS process (although not shown in Figure 6) and thus are assigned to the slow reorientation of the interface. At even lower frequencies/higher temperatures, a parallel behavior of G' and G'' is observed with an $\omega^{1/2}$ dependence. The $\omega^{1/2}$ dependence has been suggested by a number of fundamentally different theoretical approaches. In the study by Ru-

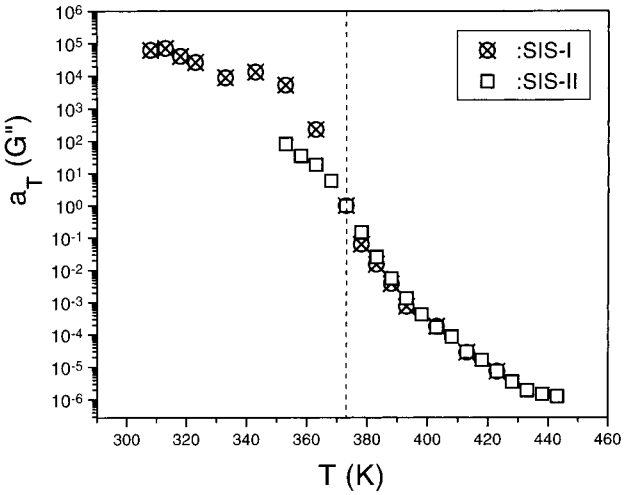

Figure 9. Temperature dependence of the shift factors ($a_T^{G''}$, T_{ref} = 373 K) for SIS-I (⊗) and SIS-II (□). Notice the weak T-depencence below the PS glass transition. The dashed line indicates the reference temperature.

binstein and Obukhov,[30] this low-frequency response was attributed to the collective diffusion of copolymer chains along the interface which is controlled by defects in lamellar orientation. Kawasaki and Onuki[31] proposed that overdamped second-sound modes in an orientationally disordered lamellar phase could result in $G^* \approx (i\omega)^{1/2}$.

Similar results have been obtained for the SIS-II (Figure 8) although over a smaller temperature range. The moduli at low frequencies/high temperatures exhibit somewhat stronger frequency dependencies (2/3 and 3/4) without displaying a true terminal response (i.e., $G' \approx \omega^2$ and $G'' \approx \omega$). The shift factors ($a_T^{G''}$), used to superimpose the G'' data, are plotted separately in Figure 9 as a function of temperature. There is a weak T-dependence of a_T at $T < T_g^{PS}$ reflecting a weak activation energy and/or overlapping processes. This situation is altered at $T > T_g^{PS}$, where a much stronger T-dependence exists (which can be described by the empirical Williams−Landel−Ferry equation) implying that the primitive friction in the microphase separated system is controlled by the PS segments.

Our main task here is to compare the results from rheology and DS with emphasis on changes occurring near and below the polystyrene T_g. For this purpose we have included in Figure 6, the $a_T(T)$ for SIS-II which is scaled to the frequency axis, from the position of G''_{max} at the reference temperature (T_{ref} = 373 K). In the same figure we show the dynamics of homopolystyrene (solid line) (Table 1) measured also by DS. Clearly, at $T > T_g^{PS}$ the shift factors obtained from rheology agree very well with the DS relaxation times of the homopolymer and of the PS-like process in SIS-I and SIS-II from DS, whereas at $T < T_g^{PS}$ the characteristic time scales probed rheologically are much longer than the dielectric process associated with the junction point fluctuations at the interface. It is therefore the *selectivity of DS* that makes possible to observe and study this new process. Over the same T-range, rheology is dominated by the dynamics of all normal modes (in DS the first normal mode dominates), of entanglements and by the network-like structure of the bridging PI midblock. These overlapping processes create the broad plateau indicated as (2) in Figure 7.

V. Conclusions

We have studied the local and global dynamics of bulk PS−PI−PS triblock copolymers in the lamellar phase using dielectric spectroscopy and rheology. Four dielectrically active processes were found, which, starting from low temperatures, reflect (i) the PI segmental dynamics, (ii) the suppressed, but yet measurable PI chain relaxation (i.e., normal modelike process), (iii) the PS-like segmental relaxation, and (iv) a slower mode associated with the reorientation of the interface. Although modes i, iii, and iv were expected based on earlier experience from microphase separated block copolymers, the existence of a measurable chain mode for tethered PI chains was, at first sight, unexpected. This process, however, can be understood in terms of the mobility of the junction point within the interface. From the dielectric strength of this process an estimate of the mean-square fluctuations of the junction points is given (in the order 4−6 nm), which is in good agreement with independent calculations of the interfacial width based on the thermodynamic interaction parameter. Dielectric spectroscopy can, therefore, be used as a *dynamic probe of the interface* in ordered triblock copolymers. These results are generalized for various nonlinear block copolymers with a basic triblock.[32] Rheology provides a broad spectrum of modes from entangled PI chains below the PS glass transition and the PS-segmental relaxation and slower modes associated with the interface at higher temperatures.

Acknowledgment. This work was supported by the Alexander von Humboldt-Stiftung. We thank Professor A. N. Semenov for helpful discussions. I.A. thanks FORTH's Institute of Electronic Structure and Laser for the hospitality.

References and Notes

(1) For a recent review: Colby, R. H. In *Curr. Opin. Colloid Interface Sci.* **1996**, *1*, 454.
(2) Helfand, E.; Tagami, Y. *J. Chem. Phys.* **1971**, *56*, 3592; *J. Polym. Sci. B* **1971**, *9*, 741.
(3) Broseta, D.; Fredrickson, G. H.; Helfand, E.; Leibler, L. *Macromolecules* **1990**, *23*, 132.
(4) Semenov, A. N. *Macromolecules* **1993**, *26*, 6617.
(5) Leibler, L. *Macromolecules* **1980**, *13*, 1602.
(6) Olvera de la Cruz, M.; Sanchez, I. C. *Macromolecules* **1986**, *19*, 2501.
(7) Floudas, G.; Hadjichristidis, N.; Iatrou, H.; Pakula, T.; Fischer, E. W. *Macromolecules* **1994**, *27*, 7735.
(8) Floudas, G.; Pispas, S.; Hadjichristidis, N.; Pakula, T.; Erukhimovich, I. Ya. *Macromolecules* **1996**, *29*, 4142.
(9) Erukhimovich, I. Ya. *Vysokomol. Soedin* **1982**, *A24*, 1950 (translated in *Polym. Sci. USSR (Engl. Transl.)* **1982**, *24*, 2232).
(10) Mayes, A. M.; Olvera de la Cruz, M. *J. Chem. Phys.* **1989**, *91*, 7228.
(11) Mayes, A. M.; Olvera de la Cruz, M. *J. Chem. Phys.* **1991**, *95*, 4670.
(12) Han, C. D.; Baek, D. M.; Kim, J. K. *Macromolecules* **1990**, *23*, 561.
(13) Gehlsen, M. D.; Almdal, K.; Bates, S. F. *Macromolecules* **1992**, *25*, 939.
(14) Riise, B. L.; Fredrickson, G. H.; Larson, R. G.; Pearson, D. L. *Macromolecules* **1995**, *28*, 7653.
(15) Matsushita, Y.; Nomura, M.; Watanabe, J.; Mogi, Y.; Noda, I.; Imai, M. *Macromolecules* **1995**, *28*, 6007.
(16) Hadziioannou, G.; Mathis, A.; Skoulios, A. *Colloid Polym. Sci.* **1979**, *257*, 136.
(17) Morrison, F. A.; Winter, H. H. *Macromolecules* **1989**, *22*, 3533.
(18) Morrison, F. A.; Winter, H. H.; Gronski, W.; Barnes, J. D. *Macromolecules* **1990**, *23*, 4200.
(19) Pakula, T.; Saijo, K.; Kawai, H.; Hashimoto, T. *Macromolecules* **1985**, *18*, 1294.
(20) Pakula, T.; Saijo, K.; Hashimoto, T. *Macromolecules* **1985**, *18*, 2037.

(21) Sakurai, S.; Momii, T.; Taie, K.; Shibayama, M.; Nomura, S.; Hashimoto, T. *Macromolecuels* **1993**, *26*, 485.
(22) Nakatani, A. I.; Morrison, F. A.; Douglas, J. F.; Mayes, J. W.; Jackson, C. L.; Muthukumar, M.; Han, C. C. *J. Chem. Phys.* **1996**, *104*, 1589.
(23) Adams, L. J.; Graessley, W. W.; Register, R. A. *Macromolecules* **1994**, *27*, 6026.
(24) Watanabe, H. *Macromolecules* **1995**, *28*, 5006.
(25) Stockmayer, W. H. *Pure Appl. Chem.* **1967**, *15*, 539. Bauer, M. E.; Stockmayer, W. H. *J. Chem. Phys.* **1965**, *43*, 4319. Stockmayer, W. H.; Burke, J. J. *Macromolecules* **1969**, *2*, 647.
(26) (a) Adachi, K.; Kotaka, T. *Prog. Polym. Sci.* **1993**, *18*, 585. (b) Adachi, K.; Kotaka, T. *Macromolecules* **1985**, *18*, 466. (c) Adachi, K.; Kotaka, T. *Macromolecules* **1988**, *21*, 157. (d) Boese, D.; Kremer, F. *Macromolecules* **1990**, *23*, 829. (e) Yao, M.-L.; Watanabe, H.; Adachi, K.; Kotaka, T. *Macromolecules* **1991**, *24*, 2955. (f) Stuhn, B.; Stickel, F. *Macromolecules* **1992**, *25*, 5306. (g) Floudas, G.; Hadjichristidis, N.; Iatrou, H.; Pakula, T. *Macromolecules* **1996**, *29*, 3139. (h) Karatasos, K.; Anastasiadis, S.; Floudas, G.; Fytas, G.; Pispas, S.; Hadjichristidis, N.; Pakula, T. *Macromolecules* **1996**, *29*, 1326. (i) Sakamoto, N.; Hashimoto, T.; Kido, R.; Adachi, K. *Macromolecules* **1996**, *29*, 8126. (j) Alig, I.; Kremer, F.; Fytas, G.; Roovers, J. *Macromolecules* **1992**, *25*, 5277.
(27) Morton, M.; Fetters, L. *J. Rubber Chem. Technol.* **1975**, *48*, 359.
(28) Iatrou, H.; Hadjichristidis, N. *Macromolecules* **1992**, *25*, 4649.
(29) Iatrou, H.; Hadjichristidis, N. *Macromolecules* **1993**, *25*, 2479.
(30) Rubinstein, M.; Obukhov, S. P. *Macromolecules* **1993,** *26*, 1740.
(31) Kawasaki, K.; Onuki, A. *Phys. Rev. A* **1990**, *42*, 3664.
(32) Floudas,G.; Alig, I.; Avgeropoulos, A.; Hadjichristidis, N. *J. Non-Cryst. Solids* (submitted).

MA970101Q